HEPATOLOGY

GATA4 loss in hepatic stellate cells cause liver fibrosis

Journal:	*Hepatology*
Manuscript ID:	HEP-13-1445
Wiley - Manuscript type:	Original
Date Submitted by the Author:	11-Jul-2013
Complete List of Authors:	Delgado, Irene; Centro Andaluz de Biología Molecular y Medicina Regenerativa (CABIMER), Cano, Elena; University of Malaga, Department of Animal Biology, Faculty of Science Carmona, Rita; University of Malaga, Department of Animal Biology, Faculty of Science García-Carbonero, Rocío; Instituto de Biomedicina de Sevilla (IBiS)-Hospital Universitario Virgen del Rocío/Consejo Superior de Investigaciones Científicas/Universidad de Sevilla, Oncology Unit Marín, Luis-Miguel; Virgen del Rocío Hospital, Liver Transplantation Soria, Bernat; Centro Andaluz de Biología Molecular y Medicina Regenerativa (CABIMER), Martín, Francisco; Centro Andaluz de Biología Molecular y Medicina Regenerativa (CABIMER), Cano, David; Instituto de Biomedcina de Sevilla (IBiS)-Hospital Universitario Virgen del Rocío/Consejo Superior de Investigaciones Científicas/Universidad de Sevilla, Endocrinology Unit Múñoz-Chápuli, Ramón; University of Malaga, Department of Animal Biology, Faculty of Science Rojas, Anabel; 1 Centro Andaluz de Biología Molecular y Medicina Regenerativa (CABIMER),
Keywords:	fetal liver, cirrhosis, septum transversum mesenchyme, embryonic lethality , Lhx2

GATA4 loss in hepatic stellate cells causes liver fibrosis

Irene Delgado[1], Elena Cano[2], Rita Carmona[2], Rocío García-Carbonero[3], Luis M Marín-Gómez[4], Bernat Soria[1], Francisco Martín[1], David A. Cano[5], Ramón Muñoz-Chápuli[2] and Anabel Rojas[1]*

[1] Centro Andaluz de Biología Molecular y Medicina Regenerativa (CABIMER), Sevilla, Spain. Centro de Investigación Biomédica en Red de Diabetes y Enfermedades Metabólicas Asociadas (CIBERDEM), Spain. [2] Department of Animal Biology, Faculty of Science, University of Malaga, Málaga, Spain. [3] Oncology Unit, Instituto de Biomedicina de Sevilla (IBiS), Hospital Universitario Virgen del Rocío/Consejo Superior de Investigaciones Científicas/Universidad de Sevilla, Hospital Universitario Virgen del Rocío, Sevilla, Spain. [4] Surgical Department, Instituto de Biomedicina de Sevilla (IBiS), Hospital Universitario Virgen del Rocío/Consejo Superior de Investigaciones Científicas/Universidad de Sevilla, Sevilla, Spain. [5] Endocrinology Unit, Instituto de Biomedicina de Sevilla (IBiS), Hospital Universitario Virgen del Rocío/Consejo Superior de Investigaciones Científicas/Universidad de Sevilla, Sevilla, Spain.

Key words: mesenchyme, fetal liver, embryonic lethality, cirrhosis, septum transversum, Lhx2

*Corresponding author
Avda. Americo Vespucio s/n.
Parque Científico Isla de la Cartuja
41092 Sevilla, Spain
E-mail: anabel.rojas@cabimer.es
Phone: (+34) 954 467 427
FAX: (+34) 954 461 664

Financial Support: I.D. was supported by a contract from Consejería de Salud, Junta de Andalucía (PI-0008). E. Cano is recipient of a MINECO fellowship (BES-2009-014847). This work was supported by grants from ISCIII co-funded by Fondos FEDER , PI11/01125 to AR, BFU2011-25304 (Ministerio de Economía y Competitividad), P11-CTS-7564 (Junta de Andalucía) and RD12/0019/0022 (TerCel network, ISCIII) to RMCh, Spanish Ministry of Science and Innovation (SAF2008-02469 and SAF2011-26805) and the Andalusian Regional Ministry of Economy, Science and Innovation (P08-CVI-3727) to D.A.C and Instituto de Salud Carlos III (Co-funded by FEDER: Red TerCel- Grant RD06/0010/0025; Grant PI10/00964), Consejería de Innovación Ciencia y Empresa, Junta de Andalucía (Grant CTS-6505), Ministry of Health and Consumer Affairs (Advanced Therapies Program Grant TRA-120), European Union: BIOREG SOE3/P1/E750 (Con-funded by FEDER) to B.S.

Abbreviations:

DAPI: 4,6-diamidino-2-phenylindole

E: embryonic day

ECM: Extracellular matrix

FACS: fluorescent-activated cell sorting

HSCs: Hepatic Stellate Cells

H&E: Hematoxylin and eosin

PHH3: Phospho-Histone H3

SMA: smooth muscle alpha actin

STM: septum transversum mesenchyme

WT: wild type

YFP: Yellow fluorescent protein

Abstract

The zinc finger transcription factor GATA4 controls specification and differentiation of multiple cell types during embryonic development. In mouse embryonic liver, GATA4 is expressed in the endodermal hepatic bud and in the adjacent mesenchyme of the septum transversum. Previous studies have shown that *Gata4* inactivation impairs liver formation. However, whether these defects are caused by loss of *Gata4* in the hepatic endoderm or in the septum transversum mesenchyme remains to be determined. In this study, we have investigated the role of mesenchymal GATA4 activity in liver formation. To that end, we generated a Cre-expressing transgenic mouse line to specifically target the septum transversum mesenchyme and its derivatives. *Conclusions:* Conditional inactivation of *Gata4* in hepatic mesenchymal cells leads to embryonic lethality around mouse embryonic stage 13.5 likely as a consequence of fetal anemia. *Gata4* KO fetal livers exhibit reduced size, advanced fibrosis, accumulation of extracellular matrix components (ECM) and hepatic stellate cells (HSCs) activation. Haploinsufficiency of *Gata4* enhances and accelerates the CCl_4-induced liver fibrosis in adult mice. Moreover, we have found that *Gata4* expression is dramatically reduced in advanced hepatic fibrosis and cirrhosis in humans. Our data demonstrate that mesenchymal GATA4 activity regulates HSCs activation and inhibits the liver fibrogenic process. Our findings suggest that activating *Gata4* expression in HSCs may provide a novel therapeutic approach for human liver fibrosis.

Introduction

Liver fibrosis is a pathophysiological response to chronic injuries produced mainly by alcohol abuse, virus infection or bile duct obstruction. A common characteristic to all types of liver fibrosis is the transformation of quiescent hepatic stellate cells (HSCs) into an active and proliferative myofibroblastic phenotype. Activated HSCs are the main source of liver extracellular matrix components (ECM), such as collagen and laminin, that form the fibrotic scars (1). Liver fibrosis can be reversed if the insult that initiated it is removed. The regression of liver fibrosis implies breakdown of ECM by metalloproteinases and the clearance of activated HSCs by apoptosis or reversion to an inactive phenotype (2). However, if the injury is sustained liver fibrosis can progress and leads to cirrhosis, which is marked by an excessive accumulation of ECM, distorted liver architecture and impairment of hepatic function. Currently, one of the emerging therapies for liver fibrosis focuses in the inhibition of HSCs activation and proliferation (3, 4). Although much is known about the signals that trigger HSCs activation in liver fibrosis, the transcription factors that mediate this process are relatively unknown.

GATA4 is a member of the zinc finger transcription factor family that is expressed in various mesoderm- and endoderm-derived tissues (5). Inactivation of *Gata4* in the germ line leads to embryonic lethality as a result of defects in extraembryonic endoderm (6-8). During mouse development, GATA4 is expressed in the foregut endoderm that eventually will form the hepatic bud, and in the adjacent lateral mesoderm at embryonic day (E) 8.0. By E9.0, the endodermal cells delaminate from the hepatic bud and migrate into the septum transversum mesenchyme (STM) differentiating into the hepatic lineages. During this developmental stage, *Gata4*

expression is not longer detected in the delaminating hepatoblast, but it is strongly maintained in the septum transversum (9). At later stages of embryonic development and in adult liver GATA4 expression is restricted to the mesenchyme surrounding the liver and non-parenchymal cells (10, 11). Previous studies have shown that *Gata4* inactivation impairs liver formation. However, these studies were performed in *Gata4* tetraploid embryos to circumvent the embryonic lethality of the conventional *Gata4* knockout mice. Thus, whether these defects are caused by loss of *Gata4* in the hepatic endoderm or in the septum transversum mesenchyme remains to be determined. In this study, we have investigated the role of mesenchymal GATA4 activity in liver formation by conditionally inactivating *Gata4* in the STM and its derivatives.

Experimental Procedures

Mice

Gata4 $^{flox/flox}$, *ROSA26RlacZ* and *ROSA26RYFP* mice and strategies for genotyping has been previously described (12-15).

A 642 bp fragment containing the minimal promoter from the mouse *Mef2c* gene (16) was cloned into a plasmid containing the *Cre* cDNA and the SV40 splice and polyA signal sequence. A 817 bp fragment containing the conserved region CR2 of the previously identified mouse G2 *Gata4* enhancer (10) was then cloned into the Cre expression vector to generate *Gata4* G2-Cre transgene. Transgenic mice were generated as previously described (10). *Gata4* $^{flox/flox}$ littermates were used as control mice in all experiments. All mouse experiments complied with institutional guidelines, and were reviewed and approved by the Institutional Animal Care and Use Committee (IACUC) of the University of Sevilla, Spain.

Histology, Immunohistochemistry and Immunofluorescence

Whole mount or dissected organs (embryonic and adult stages) were fixed in 4% paraformaldehyde in phosphate-buffered saline (PBS) at 4ºC overnight and processed for paraffin embedding in a Leica ASP200S tissue processor. ß-galactosidase detection was performed as previously described (10). Immunohistochemical and immunofluorescence analysis were performed as previously described (17). The following primary antibodies were used at the indicated dilutions: mouse anti-GATA4 (1:100; Santa Cruz Biotechnology, Santa Cruz, USA, Sc- 25310); rabbit anti-GATA4 (1:50, Abcam, UK, ab84593), rabbit anti-Wilms' Tumor 1(1:100; Dako, Glostrup, Denmark, 356101), rabbit anti-Collagen IV (1:400, Abcam, UK, ab19808), mouse anti-

desmin (1:50, Sigma-Aldrich, Steinheim, Germany, Clone DE-U-10, D1033), rabbit anti-laminin (1:50; Sigma-Aldrich, Steinheim, Germany, L9393), mouse smooth muscle α-actin (1:300, Sigma-Aldrich, Steinheim, Germany, A5228), rabbit anti Phospho-Histone H3 (1:500, Millipore, Billerica, MA, USA, 06-570), rabbit anti-GFP (1:50, Life Technologies, Carlsbad, California, USA, A11122), goat anti-GFP (1:200, Abcam, Cambridge, UK, ab6673), mouse anti-GFAP (1:200, DAKO, Carpinteria, California, USA), cleaved caspase-3 antibody (1:200, Cell Signaling, Massachusets, USA, 9661) Counterstaining with DAPI (4,6-diamidino-2-phenylindole; Sigma Aldrich, Steinheim, Germany, 32670) was perfomed to reveal nuclei. Secondary antibodies coupled to Alexa-488, Alexa-568 (Molecular Probes), FITC, and Cy3- (Jackson Immunoresearch) were used. Staining for diaminobenzidine (DAB) was performed with the Elite ABC kit (Vector Laboratories). Sirius red stain was performed as described (18).

Quantitative RT-PCR

Total ARN from mouse livers was isolated using RNeasy Plus Micro kit (Qiagen, Hilden, Germany, 74034) cDNA was synthesized using QuantiTect Reverse Transcription Kit (Qiagen, Hilden, Germany, 205311). Quantitative RT-PCR analysis was performed using FastStart Universal SYBR Green Master (ROCHE, 04913850001) using a 7900HT Real-Time PCR system (Applied Biosystems). RNA expression of target genes was normalized based on comparison to *β-actin* expression. The ΔΔCt method was used to calculate changes in gene expression levels. Primer sequences are shown in Supporting Table 2. Total RNA was extracted from 10-13 slices (20 µm thickness) of biopsies of human livers using mirVana miRNA islolation kit (Ambion, 1560). Expression levels of human *GATA4* and *β-ACTIN*, was performed using commercial Taqman probe sets (*GATA4* Hs00171403_m1 and *β-ACTIN*

Hs03023880_g1) (Applied Biosystems, Foster City, CA, USA).

Electrophoretic mobility shift assay (EMSA)

DNA binding reactions and generation of recombinant GATA4 protein were performed as described previously (19). The sense strand sequence of the mouse *Lhx2* GATA sites used for EMSA were: *Lhx2* G1/G2: 5´gggaatggtatatcagcgtcaactatcgcttcctctgctg-3´; *Lhx2* G3: 5-ggggagggtgcccatgtttatcaccgagtgagatg-3´. Control (+C) and mutant control oligos (-C) for GATA sites have previously been described (*Pdx1* G2 sites) (20).

CCl_4-induced fibrosis

Liver fibrosis was induced in 8-week-old *Gata4*$^{flox/+}$*;* G2-Cre and *Gata4*$^{flox/+}$control mice by intraperitoneal injections of 0.5 mL/kg CCl_4 dissolved in olive oil (1:1) twice a week. Mice received a total of five injections and were sacrificed 72 h after the last injection.

Human samples

Human liver samples were obtained from liver biopsies and from explanted fibrotic or cirrhotic livers due to transplantation. An informed consent in writing was obtained from each patient of the study. The study protocol was approved by the ethics committee of the Hospital Universitario Virgen del Rocío (HUVR), Seville and the study was conducted according to the principles of the Declaration of Helsinki. Samples were classified by a pathologist according to METAVIR score (21) as: F0, no fibrosis; F1, portal fibrosis without septa; F3, numerous septa without cirrhosis; F4, cirrhosis. Immunohistochemistry for GATA4 was performed on 4 μm paraffin sections of human liver from seven patients with no fibrosis or mild fibrosis (F0-F1) and eight patients

with moderate or severe fibrosis (F3-F4). Quantitative *GATA4* expression was determined by quantitative PCR in liver samples of six patients with no fibrosis or mild fibrosis (F0-F1) and five patients with moderate or severe fibrosis (F3-F4). Liver fibrotic samples of different etiologies were included in the study: hepatitis C viral infection, alcoholic liver disease and primary biliary cirrhosis.

Statistical Analysis

All values are expressed as mean ± SEM. Statistical analyses were performed using two tailed Student´s t-test. A p value <0.05 was considered statistically significant.

Results

Generation of a Cre-expressing mouse strain to target STM and its derivatives

Gata4 expression in the STM is controlled by a distal conserved sequence element, named *Gata4* CR2 (10). To target STM and its derivatives, we generated a transgenic mouse line in which the expression of Cre recombinase is controlled by the *Gata4* CR2 enhancer (G2-Cre mice). To examine the activity of Cre recombinase in vivo, G2-Cre mice were crossed to *ROSA26RLacZ* and *ROSA26RYFP* mice (13, 14). A total of 4 founder mice carrying the *Gata4* G2-Cre transgene were generated. Similar patterns of Cre activity were observed in all the founder lines (data not shown). Analysis of G2-Cre; *ROSA26RlacZ* embryos revealed robust ß-*galactosidase* activity in the lateral mesoderm beginning at embryonic day 8.5 (E8.5) and in the STM at E9.5 (Fig. 1A), consistent with the previously reported expression of the *Gata4-G2-lacZ* transgene (10). Similarly, strong YFP staining was found in the mesenchyme surrounding the endodermal hepatic bud in G2-Cre; *ROSA26RYFP* embryos at E9.5 **(**Supplemental Fig. 1). By E13.5, ß-galactosidase activity was observed in the liver capsule and in non-parenchymal liver cells (Fig. 1A). At that stage Cre-dependent YFP expression was also detected in the epicardium, indicating that *Gata4*-expresing cells from the septum transversum mark the proepicardial cells that will give rise to the epicardium during cardiac development (Supplemental Fig.1).

To identify the mesenchymal hepatic cells marked by the activity of the *Gata4 G2-Cre* transgene, colocalization analysis of YFP expression with different hepatic markers were performed in E11.5 *G2-Cre; ROSA26RYFP* embryos. Endogenous GATA4 protein was found in all YFP-expressing cells, indicating that *Gata4* expression is maintained during the delamination of cells from the liver mesothelium (Fig. 1B).

The majority of YFP^+ cells coexpressed Wilms' tumor 1 (WT1), a marker of liver mesothelial cells at E11.5 (22) (Fig.1B). WT1-expressing cells have been shown to give rise to hepatic stellate cells (22, 23). In agreement with this observation, most of YFP^+ cells coexpressed the HSCs marker glial fibrillary acidic protein (GFAP) (Fig. 1B). No significant contribution of *Gata4*-positive cells to hematopoietic cells was observed, as determined by flow cytometry analysis of YFP^+ cells with different hematopoietic lineage markers (megakaryocytes, leukocytes and erythrocytes) (data not shown). Endothelial cells constituted a minority of the YFP^+ population in the liver, as assessed by panendothelial cell antigen (Meca 32 clone) staining (Fig.1B). Of note, no YFP^+ cells expressed the liver epithelial marker HNF1, confirming the specificity of the Cre line to the mesodermal component of the liver (data not shown). Our results show that *Gata4*-G2-Cre mouse strain efficiently targets the STM and its derivatives.

Inactivation of Gata4 in hepatic mesenchymal cells results in embryonic lethality and liver hypoplasia

To analyze the role of mesenchymal GATA4 activity in liver formation, *Gata4* was specifically inactivated in the lateral mesoderm by crossing *Gata4* $^{flox/flox}$ mice to the G2-Cre line (hereafter; *Gata4* KO mice). Efficient excision of the *Gata4* floxed allele in the STM derivatives was confirmed by PCR of genomic DNA (Fig. 2A). Remarkably, these crosses did not yield *Gata4* KO offspring, indicating that GATA4 activity in the STM and/or its derivatives is crucial for embryonic development (Supplemental Table 1). To determine the onset of embryonic lethality, *Gata4* KO embryos were analyzed at different stages of development. At E11.5, *Gata4* KO embryos display a normal gross appearance and were present at normal Mendelian frequencies (data not shown and Supplemental Table 1). However, by E13.5, the

number of *Gata4* KO embryos was underrepresented (Supplemental Table 1). At this stage, the *Gata4* KO embryos exhibited slight growth retardation and pale appearance, indicative of anemia (Fig. 2B).

It has been previously shown that *Gata4*$^{-/-}$ tetraploid embryos display hypoplastic ventricular myocardium. A lack of proepicardium has been suggested to be the primary cause for these myocardial effects in *Gata4*$^{-/-}$ tetraploid embryos (9). To determine whether the embryonic lethality of *Gata4* KO mice might be caused by heart defects, we examined cardiac formation in conditional *Gata4* KO E13.5 embryos. The size of *Gata4* KO hearts was similar to those of control embryos (Supplemental Figure 1). Moreover, histological analyses of *Gata4* KO hearts revealed normal morphology of the epicardium and normal myocardial ventricular wall thickness (Supplemental Figure 1). These results suggest that *Gata4* loss in the epicardium does not have a detrimental effect in early cardiac development.

Next, we set out to determine whether *Gata4* inactivation in the STM might have a detrimental effect in liver formation. Gross morphological analysis revealed a dramatic reduction in liver mass in *Gata4* KO embryos (Fig. 2B). However, histological analysis of *Gata4* KO livers did not reveal major defects in hepatic endoderm morphology (see below) (Fig. 2C). Furthermore, hepatocytes expressed mature liver markers such as HNF1ß and Albumin (Fig. 2C), indicating normal hepatocyte differentiation in the absence of GATA4. To elucidate the mechanisms leading to decreased liver size, we assayed proliferation of liver cells by Phospho-Histone H3 (PHH3) immunostaining. A significant reduction of proliferating cells was observed in *Gata4* KO livers compared with control livers at E13.5 (Fig. 3A, B). Concomitant with

the reduced proliferation of liver cells, we observed a noticeable increase in apoptotic cells in *Gata4* KO livers (Fig. 3A, B). During mouse embryonic development, the liver serves as hematopoietic organ from E10.5 to postnatal stages. The pale aspect of the *Gata4* KO embryos was suggestive of severe anemia that could be the cause of the observed embryonic lethality. Thus, we examined fetal liver hematopoiesis in E12.5 *Gata4* KO embryos livers by flow cytometry analysis with markers of the different hematopoietic cell types. These experiments revealed a dramatic decrease in hematopoietic cells in *Gata4* KO livers (Supplemental Fig. 2). Taken together, these results indicate that loss of GATA4 in the septum transversum and/or its derivatives impairs fetal hematopoiesis and liver growth.

Accumulation of ECM, activation of hepatic stellate cells and fibrosis induction in Gata4 KO embryos

The architecture of the liver of the *Gata4* KO embryos was distorted with the presence of fibrous-like tissue surrounding the lobules, suggesting an ongoing fibrotic process (Fig. 2B). Further histological analysis revealed dispersed hepatocytes with sinusoidal spaces filled by collagen fibers in E13.5 *Gata4* KO fetal livers (Fig. 4A, B). Immunohistochemical analysis revealed a marked increase of the basement membrane components laminin and Collagen type IV in *Gata4* KO livers, indicating that the inactivation of *Gata4* leads to accumulation of extracellular matrix (ECM) (Fig. 4C-F). Collagen and laminin are synthesized mainly by proliferative and active HSCs (24). Indeed, a dramatic increase in the number of cells expressing the HSC-specific marker desmin was observed in *Gata4* KO livers (Fig. 5A), indicating that GATA4 loss induces HSCs proliferation. Moreover, HSCs in the *Gata4 KO* livers displayed an active myofibroblast phenotype, characterized by the high levels of smooth muscle α-actin

(SMA) expression, a hallmark of liver fibrosis (25) (Fig. 5A). Quantitative RT-PCR analysis confirmed the increased expression of HSCs markers *Desmin* and *Sma* in *Gata4* KO livers (Fig. 5B). Previous studies have suggested the hedgehog (Hh) signaling pathway promotes the growth of HSC populations (26). In agreement with these reports, increased expression of the Hh ligand *Shh* (Fig. 5B) was found in *Gata4* KO livers.

The liver abnormalities in *Gata4* KO embryos closely resemble those observed in mice deficient in the transcription factor Lhx2 (27). We therefore measured the *Lhx2* expression in *Gata4* KO fetal livers by quantitative RT-PCR. A significant decrease in *Lhx2* expression was observed in *Gata4* KO livers (Fig. 5B). These results raised the question of whether GATA4 might directly regulate *Lhx2* expression. Bioinformatics analyses revealed three evolutionary conserved GATA sites in the *Lhx2* promoter region, named as G1, G2 and G3, at positions -3411, -3398 and -3340, respectively. These sites were bound efficiently by recombinant GATA4 protein in EMSA experiments (Fig. 5C, D), suggesting that GATA4 might act as a direct transcriptional regulator of *Lhx2* in HSCs. Altogether, these results indicate that in the absence of GATA4 HSCs acquire an active state inducing a fibrogenic process.

Gata4 haploinsufficiency exacerbates CCl_4-induced fibrosis

Our previous findings in *Gata4* KO embryos raise the question of whether GATA4 loss may cause liver fibrosis in adult stages. Since the embryonic lethality *Gata4* KO mice precluded an analysis of liver function in adult mice, we examined conditional heterozygous *Gata4*$^{flox/+}$; G2-Cre mice (hereafter, *Gata4* Het mice). Gross morphological examination and histological analysis of liver tissue did not reveal

obvious defects in adult *Gata4* Het livers (data not shown). To test whether *Gata4* haploinsufficiency might have an effect in HSCs activation upon liver injury, *Gata4* Het mice were treated with repeated subcutaneous injections of carbon tetrachloride (CCl_4), a widely used model for liver fibrosis (28, 29). We used a short-term CCl_4 treatment to induce moderate liver fibrosis. As expected, CCl_4 treatment caused a mild increase in collagen fiber production in control livers with rare thin septa (Fig. 6A, B). However, CCl_4-treated *Gata4* Het mice displayed a higher degree of liver fibrosis and numerous septa compared with CCl_4-injected control mice (Fig. 6A, B). These results indicate that haploinsufficiency of *Gata4* promotes CCl_4- induced liver fibrosis and support a role for GATA4 in maintaining the quiescent state of adult HSCs.

Down-regulation of GATA4 expression in human cirrhotic liver

The response to liver injury is well conserved between rodents and humans. To provide further evidence for the role of GATA4 in hepatic fibrosis, we examined the expression of *GATA4* in liver samples from patients with advanced liver fibrosis and cirrhosis by immunohistochemical analyses. First, we determined whether GATA4 protein was present in the mesenchymal compartment of livers from healthy individuals or patients with mild fibrosis (F0-F1 fibrosis). Similarly to what we have observed in mice, GATA4 was found in HSCs of human livers (Fig. 7A). Next, we analyzed GATA4 in livers of patients with advanced liver fibrosis of different etiologies. Staining with Sirius Red confirmed the excessive collagen deposition and bridging fibrosis characteristic of later stages of liver fibrosis (F3-F4) (Fig. 7A). Remarkably, accumulation of GATA4 protein was dramatically decreased in F3-F4 patients compared to F0-F1 patients (Fig. 7A). Quantitative analyses of *GATA4* mRNA levels confirmed the significant reduction in *GATA4* expression in patients with advanced

fibrosis (Fig.7B). These results indicate that *GATA4* expression becomes down-regulated in HSCs during the progression of liver fibrosis.

Discussion

In this study we show that inactivation of GATA4 in the hepatic mesenchyme results in severe liver hypoplasia and embryonic lethality. G*ata4* KO embyos exhibit progressive liver fibrosis associated with increased HSCs activation indicating that GATA4 activity in mesenchyme inhibits the fibrogenic process.

Previous studies using genetic lineage tracing tools have shown that the STM gives rise to liver mesenchyme (22, 30). We have previously reported that the expression of *Gata4* transcription factor in the STM is controlled by a distal conserved sequence element, named *Gata4* CR2 (10). Thus, to specifically target the STM and its derivatives, we have generated a transgenic mouse line in which Cre expression is directed by the *Gata4* CR2 enhancer. Our analysis of the G2-Cre mice reveals robust expression in the STM and the liver mesenchymal compartment during early and mid stages of embryonic development, respectively. Importantly, quiescent HSCs are efficiently targeted in the G2-Cre mice. Thus, the G2-Cre mouse strain represents a novel tool to specifically manipulate gene function in mesenchymal liver cells.

Liver bud growth is impaired in *Gata4* KO mice. However, liver bud induction and hepatocyte differentiation are not affected by loss of mesenchymal GATA4 activity. The reduced liver size of *Gata4* KO mice appears to be a consequence of diminished hepatoblast proliferation and increased apoptosis. The liver mesenchyme produces a significant number of signaling molecules that promote hepatoblast proliferation and survival (31). Thus, GATA4 might control some of these paracrine signals from the liver mesenchyme affecting hepatic endoderm growth. This defective expansion of the hepatic endoderm could explain the diminished hematopoiesis observed in *Gata4* KO

mice. The G2-Cre transgene does not target the hematopoietic stem cell compartment. Therefore, the impaired hematopoiesis in *Gata4* KO mice must be secondary to the loss of mesenchymal GATA4 activity. To this regard, it should be noted that anemia and embryonic lethality is commonly observed in mice with defects in liver formation (31).

The phenotype of *Gata4*-deficient fetal livers resembles the fibrogenic process that occurs in adult liver in response to external injury, including increased accumulation of ECM proteins and activation of HSCs. Furthermore, *Gata4* KO livers display altered expression of genes involved in HSC activation such as *Shh* (32) and the LIM homeobox gene *Lhx2*. *Gata4* KO mice phenocopy the effect of *Lhx2* inactivation, and the *Gata4* and *Lhx2* expression patterns overlap during liver embryonic development (33), suggesting a potential genetic interaction between these two transcription factors. Indeed, our electrophoretic mobility shift assay experiments indicate a direct binding of GATA4 to *Lhx2* promoter. Thus, we propose a model in which GATA4 regulates *Lhx2* expression in the hepatic mesenchyme during fetal liver development inhibiting HSCs activation and the associated fibrogenic process. Consistent with the reported expression of *Gata4* in adult liver mesenchymal cells in mice (11), our results show that mesenchymal *Gata4* activity also regulates adult liver fibrosis. Adult *Gata4* Het mice display exacerbated liver fibrosis upon CCl_4 treatment indicating that the fibrogenic response to liver injury is sensitive to decreased *Gata4* gene dosage in liver mesenchymal tissue. Although a potential function of GATA4 in human liver fibrosis remains to be determined, our observations that *GATA4* expression is reduced in livers with advanced fibrosis/cirrhosis suggest that mesenchymal GATA4 activity might also regulate liver fibrosis in humans.

In conclusion, GATA4 function in liver mesenchymal cells is important for controlling HSC activation and may represent a new potential target for therapeutic strategies in liver fibrosis.

Acknowledgments

We thank Dr. William Pu for providing the *Gata4* floxed mice. We also thank Manuel Carrasco for helpful discussion of the manuscript and Antonio Cárdenas and Raquel Araujo for their technical assistance. We are grateful to Biobanco of Hospital Virgen del Rocío. María del Pilar González Sánchez and Ana Morilla Camacho from CPYEA generated G2-Cre transgenic mice.

References

1. Bataller R, Brenner DA. Liver fibrosis. J Clin Invest 2005;115:209-218.
2. Kisseleva T, Brenner DA. Role of hepatic stellate cells in fibrogenesis and the reversal of fibrosis. J Gastroenterol Hepatol 2007;22 Suppl 1:S73-78.
3. Bataller R, Brenner DA. Hepatic stellate cells as a target for the treatment of liver fibrosis. Semin Liver Dis 2001;21:437-451.
4. Fallowfield JA. Therapeutic targets in liver fibrosis. Am J Physiol Gastrointest Liver Physiol;300:G709-715.
5. Arceci RJ, King AA, Simon MC, Orkin SH, Wilson DB. Mouse GATA-4: a retinoic acid-inducible GATA-binding transcription factor expressed in endodermally derived tissues and heart. Mol Cell Biol 1993;13:2235-2246.
6. Molkentin JD, Lin Q, Duncan SA, Olson EN. Requirement of the transcription factor GATA4 for heart tube formation and ventral morphogenesis. Genes Dev 1997;11:1061-1072.
7. Kuo CT, Morrisey EE, Anandappa R, Sigrist K, Lu MM, Parmacek MS, Soudais C, et al. GATA4 transcription factor is required for ventral morphogenesis and heart tube formation. Genes Dev 1997;11:1048-1060.
8. Narita N, Bielinska M, Wilson DB. Wild-type endoderm abrogates the ventral developmental defects associated with GATA-4 deficiency in the mouse. Dev Biol 1997;189:270-274.
9. Watt AJ, Zhao R, Li J, Duncan SA. Development of the mammalian liver and ventral pancreas is dependent on GATA4. BMC Dev Biol 2007;7:37.
10. Rojas A, De Val S, Heidt AB, Xu SM, Bristow J, Black BL. Gata4 expression in lateral mesoderm is downstream of BMP4 and is activated directly by Forkhead and GATA transcription factors through a distal enhancer element. Development 2005;132:3405-3417.
11. Zhao R, Watt AJ, Li J, Luebke-Wheeler J, Morrisey EE, Duncan SA. GATA6 is essential for embryonic development of the liver but dispensable for early heart formation. Mol Cell Biol 2005;25:2622-2631.
12. Pu WT, Ishiwata T, Juraszek AL, Ma Q, Izumo S. GATA4 is a dosage-sensitive regulator of cardiac morphogenesis. Dev Biol 2004;275:235-244.
13. Srinivas S, Watanabe T, Lin CS, William CM, Tanabe Y, Jessell TM, Costantini F. Cre reporter strains produced by targeted insertion of EYFP and ECFP into the ROSA26 locus. BMC Dev Biol 2001;1:4.
14. Soriano P. Generalized lacZ expression with the ROSA26 Cre reporter strain. Nat Genet 1999;21:70-71.
15. Rajagopal SK, Ma Q, Obler D, Shen J, Manichaikul A, Tomita-Mitchell A, Boardman K, et al. Spectrum of heart disease associated with murine and human GATA4 mutation. J Mol Cell Cardiol 2007;43:677-685.
16. Dodou E, Verzi MP, Anderson JP, Xu SM, Black BL. *Mef2c* is a direct transcriptional target of ISL1 and GATA factors in the anterior heart field during mouse embryonic development. Development 2004;131:3931-3942.
17. Rojas A, Schachterle W, Xu SM, Black BL. An endoderm-specific transcriptional enhancer from the mouse Gata4 gene requires GATA and homeodomain protein-binding sites for function in vivo. Dev Dyn 2009;238:2588-2598.
18. Junqueira LC, Bignolas G, Brentani RR. Picrosirius staining plus polarization microscopy, a specific method for collagen detection in tissue sections. Histochem J 1979;11:447-455.

19. Rojas A, Kong SW, Agarwal P, Gilliss B, Pu WT, Black BL. GATA4 is a direct transcriptional activator of cyclin D2 and Cdk4 and is required for cardiomyocyte proliferation in anterior heart field-derived myocardium. Mol Cell Biol 2008;28:5420-5431.
20. Carrasco M, Delgado I, Soria B, Martin F, Rojas A. GATA4 and GATA6 control mouse pancreas organogenesis. J Clin Invest;122:3504-3515.
21. Poynard T, Ratziu V, Benmanov Y, Di Martino V, Bedossa P, Opolon P. Fibrosis in patients with chronic hepatitis C: detection and significance. Semin Liver Dis 2000;20:47-55.
22. Asahina K, Zhou B, Pu WT, Tsukamoto H. Septum transversum-derived mesothelium gives rise to hepatic stellate cells and perivascular mesenchymal cells in developing mouse liver. Hepatology;53:983-995.
23. Ijpenberg A, Perez-Pomares JM, Guadix JA, Carmona R, Portillo-Sanchez V, Macias D, Hohenstein P, et al. Wt1 and retinoic acid signaling are essential for stellate cell development and liver morphogenesis. Dev Biol 2007;312:157-170.
24. Friedman SL, Roll FJ, Boyles J, Bissell DM. Hepatic lipocytes: the principal collagen-producing cells of normal rat liver. Proc Natl Acad Sci U S A 1985;82:8681-8685.
25. Rockey DC, Boyles JK, Gabbiani G, Friedman SL. Rat hepatic lipocytes express smooth muscle actin upon activation in vivo and in culture. J Submicrosc Cytol Pathol 1992;24:193-203.
26. Yang L, Wang Y, Mao H, Fleig S, Omenetti A, Brown KD, Sicklick JK, et al. Sonic hedgehog is an autocrine viability factor for myofibroblastic hepatic stellate cells. J Hepatol 2008;48:98-106.
27. Wandzioch E, Kolterud A, Jacobsson M, Friedman SL, Carlsson L. Lhx2-/- mice develop liver fibrosis. Proc Natl Acad Sci U S A 2004;101:16549-16554.
28. Constandinou C, Henderson N, Iredale JP. Modeling liver fibrosis in rodents. Methods Mol Med 2005;117:237-250.
29. Weiler-Normann C, Herkel J, Lohse AW. Mouse models of liver fibrosis. Z Gastroenterol 2007;45:43-50.
30. Asahina K, Tsai SY, Li P, Ishii M, Maxson RE, Jr., Sucov HM, Tsukamoto H. Mesenchymal origin of hepatic stellate cells, submesothelial cells, and perivascular mesenchymal cells during mouse liver development. Hepatology 2009;49:998-1011.
31. Zorn AM. Liver development. 2008.
32. Omenetti A, Choi S, Michelotti G, Diehl AM. Hedgehog signaling in the liver. J Hepatol;54:366-373.
33. Kolterud A, Wandzioch E, Carlsson L. Lhx2 is expressed in the septum transversum mesenchyme that becomes an integral part of the liver and the formation of these cells is independent of functional Lhx2. Gene Expr Patterns 2004;4:521-528.

Figure Legends

Figure 1. The *Gata4* G2-Cre transgene marks the lateral mesoderm, STM and its derivatives**. (A)** X-gal staining reveals Cre activity of the *Gata4* G2-Cre transgene in the lateral mesoderm (arrowheads) of G2-Cre*; ROSA26RlacZ* embryos at E8.5. Robust ß-galactosidase activity is observed in the septum transversum (st) but not in the hepatic endoderm (he) at E9.5. At midgestation (E13.5), *Gata4*$^{+}$ from the septum transversum mesenchyme contribute to liver mesenchymal cells of the sinusoids. **(B)** Labeling of the *Gata4* G2-Cre lineage in *ROSA26RYFP* mice. Liver YFP^{+} cells express GATA4 at E11.5 (arrowheads). At that stage, most of the YFP^{+} cells co-express the mesothelial marker, Wilms' tumor 1 in the mesothelium and the HSCs marker GFAP in the sinusoids (inset shows a higher magnification of GFPA/YFP^{+} cells). A few G2-Cre-marked cells are associated to blood vessels, as shown by expression of the endothelial marker panendothelial cell antigen (Meca 32 clone) (arrows). Scale bars = 50µm. Scale bar in inset = 25µm.

Figure 2. Liver hypoplasia in *Gata4* conditional knockout embryos. (A) PCR using specific primers for *Gata4* on genomic DNA from E13.5 livers demonstrates Cre-mediated excision of the *Gata4* floxed allele. **(B)** Gross morphology images showing pale appearance and reduced liver mass (arrowhead) of E13.5 *Gata4* KO embryos compared to control (Ctrl) embryos. Livers of E13.5 *Gata4* KO embryos exhibit severe hypoplasia and disorganized hepatic lobe architecture. Note the presence of fibrous-like tissue surrounding the lobules (arrow). **(C)** Immunostaining for Albumin and HNF1ß reveals normal hepatocyte differentiation in E13.5 *Gata4* KO livers. Scale bars in B= 500µm; in C= 50µm.

Figure 3. (A) Immunohistochemical staining for Phospho-Histone H3 (pHH3) on E13.5 liver sections shows a dramatic decrease in the number of proliferating cells in *Gata4* KO embryos compared with control embryos. Increase in the number of apoptotic cells in E13.5 *Gata4* KO livers, as assessed by activated caspase-3 immunostaining. **(B)** Quantification of proliferating and apoptotic cells in E13.5 livers. Six randomly selected fields from liver sections of three control embryos and three *Gata4* KO embryos were analyzed. * $p < 0.05$ (Student's *t*-test). Scale bars =100µm

Figure 4. Liver fibrosis in *Gata4* conditional knockout fetal livers. (A, B) Histological analyses of E13.5 liver sections of control (Ctrl) and *Gata4* KO embryos reveal distorted cellular organization of the hepatocytes, which are interconnected by collagen fibers that stain with Sirius red (arrows). Immunostaining for laminin **(C, D)** and collagen IV **(E, F)** on liver sections show elevated accumulation of ECM proteins in *Gata4* KO embryos compared with Ctrl embryos. Scale bars= 100µm.

Figure 5. HSCs activation in the absence of GATA4 activity. (A) Immunostaining for Desmin shows an increased number of HSCs at E13.5 *Gata4* KO livers compared with control livers. HSCs in *Gata4* KO livers express smooth muscle alpha actin (SMA), a marker of HSCs activation. **(B)** Quantitative RT-PCR analysis of the expression of *Desmin*, *SMA*, *Shh* and *Lhx2* in E13.5 livers. Results indicate relative expression levels as ratios of normalized mean gene expression in *Gata4* KO embryos

compared with control embryos (n=3 embryos from each genotype). * $p < 0.05$ (Student's *t*-test). **(C) GATA4 directly binds to the *Lhx2* promoter.** Alignment of mouse and human sequences of *Lhx2* promoter reveals three conserved perfect GATA sites (red boxes) denoted as G1, G2 and G3. Numbers indicate the position of the GATA sites relative to the *Lhx2* transcriptional start site. **(D)** EMSA with radiolabeled double-stranded oligonucleotides encompassing the *Lhx2* G1 and G2 sites (lanes 1-5) and *Lhx2* G3 site (lanes 6-10). Lanes 1 and 6 do not contain recombinant GATA4 protein. Competitions experiments were performed adding excess of unlabeled probe of itself (lanes 3, G1/G2, and 8, G3), control site (+C) (lanes 4 and 9) and control mutated site (-C) (lanes 5 and 10). Scale bars= 100µm.

Figure 6. *Gata4* conditional heterozygous mice exhibit accelerated CCl_4-mediated liver fibrosis. (A) Polarized light microscopy pictures of Sirius-red-stained E13.5 liver sections from control or *Gata4* conditional heterozygous mice (*Gata4* Het) treated with oil or CCl_4. **(B)** Quantification of collagen fiber area in E13.5 livers. Collagen fiber area was measured as the percentage of the Sirius-red-stained area to total liver area using the image analysis software Metamorph. Six randomly selected fields were chosen per embryo. Ctrl oil, n=3; *Gata4* Het oil n=4; Ctrl CCl_4; n=8; *Gata4* Het CCl_4 =7. * $p < 0.01$ (Student's *t*-test). Scale bars = 50µm.

Figure 7. Decreased *GATA4* expression in human advanced liver fibrosis. (A) Sirius red staining and immunostaining using anti-GATA4 antibody in human liver sections from healthy/mild fibrotic livers (F0-F1) or livers with advanced liver fibrosis/cirrhosis (F3-F4). Note the decrease in *Gata4*-expressing cells in livers with advanced liver

fibrosis/cirrhosis (F3-F4) compared with healthy/mild fibrotic human livers (arrowheads). **(B)** Quantitative RT-PCR analysis of *Gata4* expression in human livers. Results indicate relative expression levels as ratios of normalized mean gene expression in livers with advanced fibrosis/cirrhosis compared to F0-F1 livers. * $p < 0.05$ (Student's *t*-test). Scale bars= 50μm.

Delgado et al., Figure 1

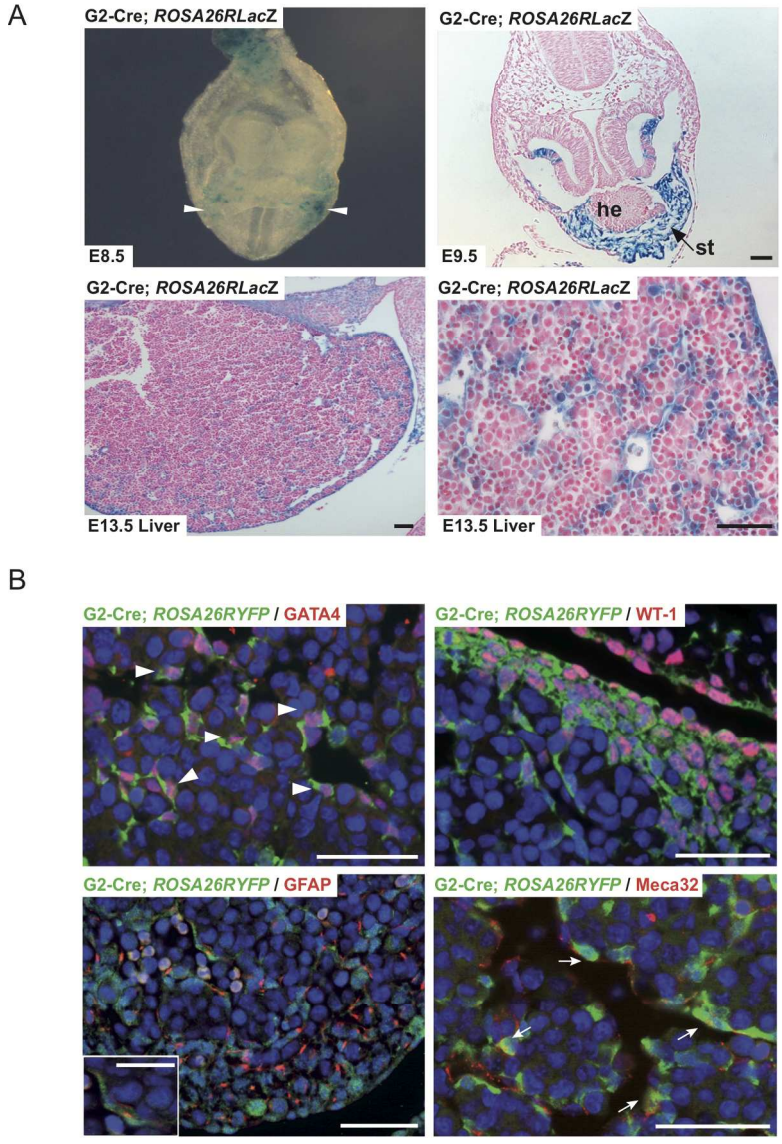

144x224mm (300 x 300 DPI)

Delgado et al., Figure 2

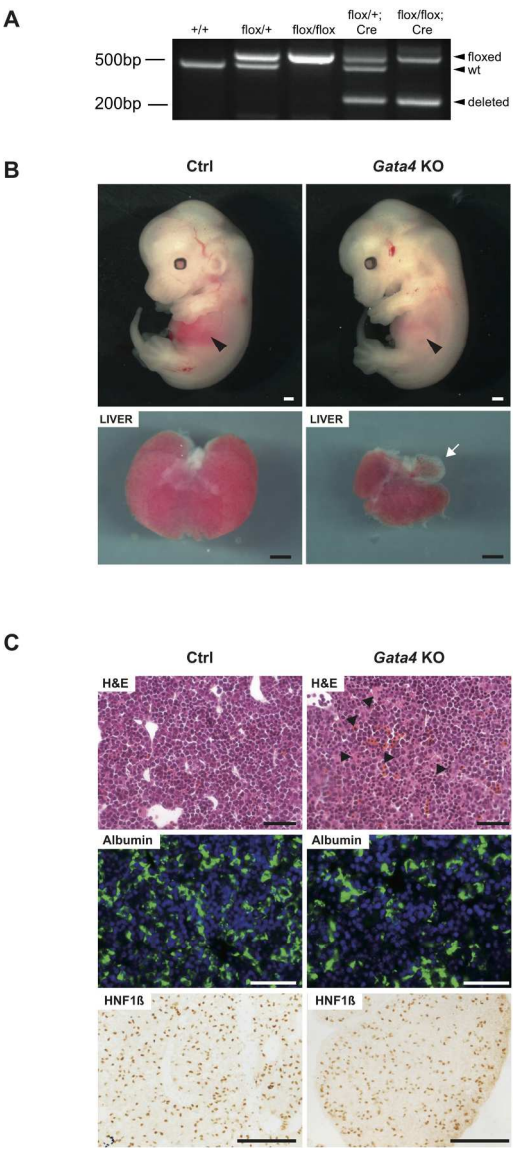

110x260mm (300 x 300 DPI)

Delgado et al., Figure 3

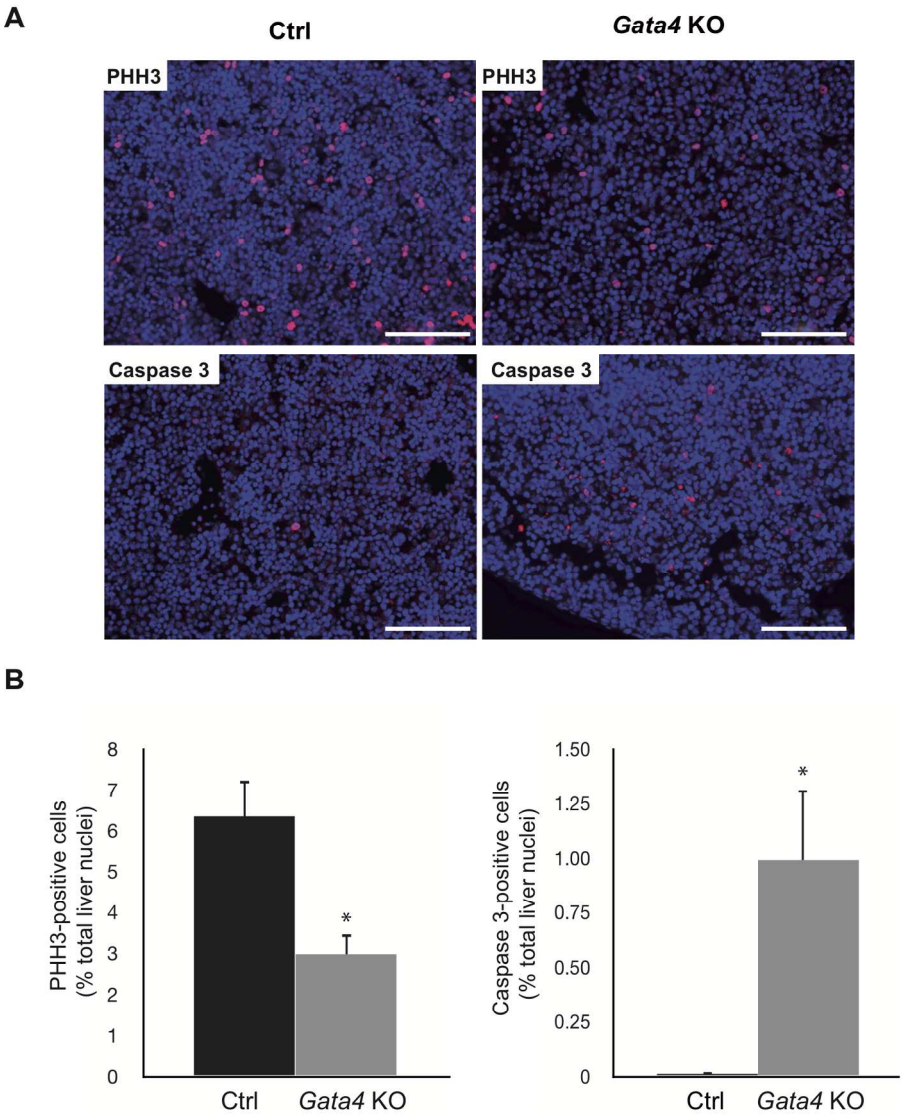

153x203mm (300 x 300 DPI)

Delgado et al., Figure 4

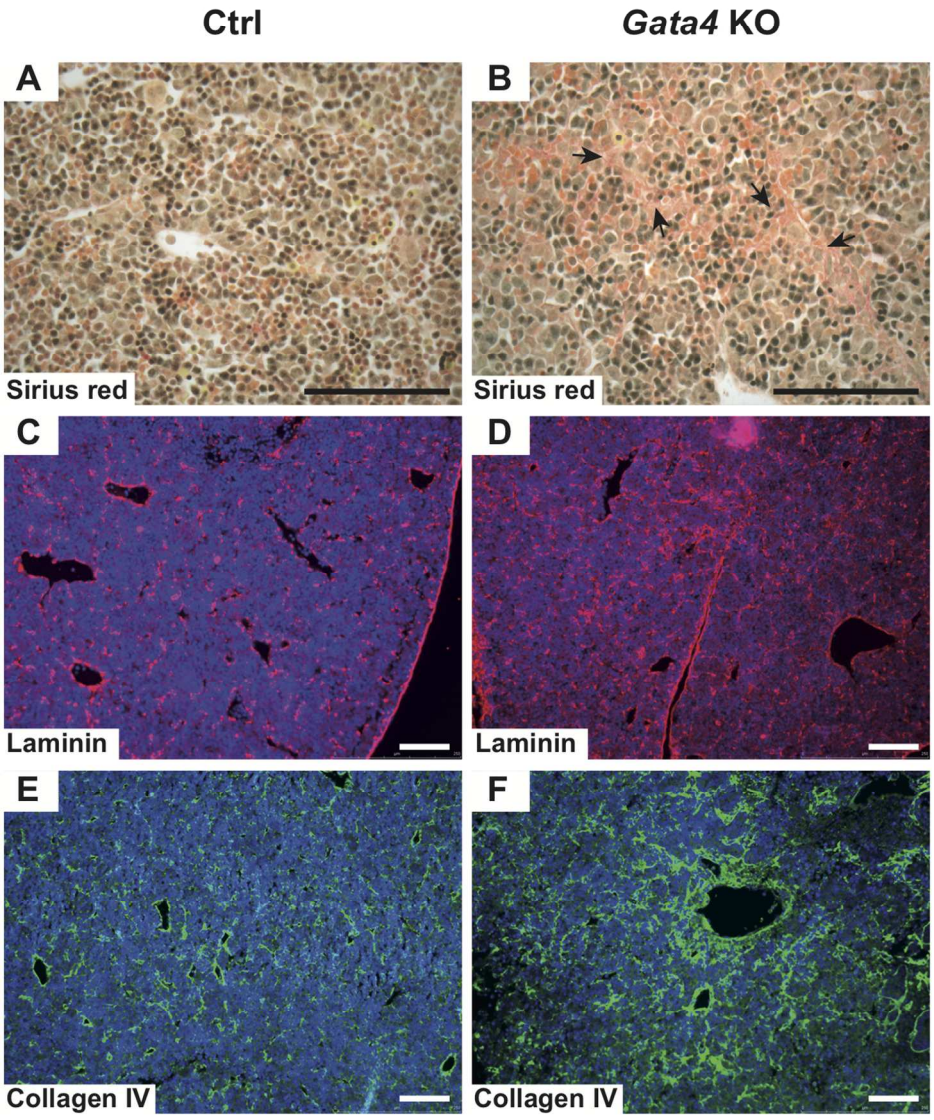

111x144mm (300 x 300 DPI)

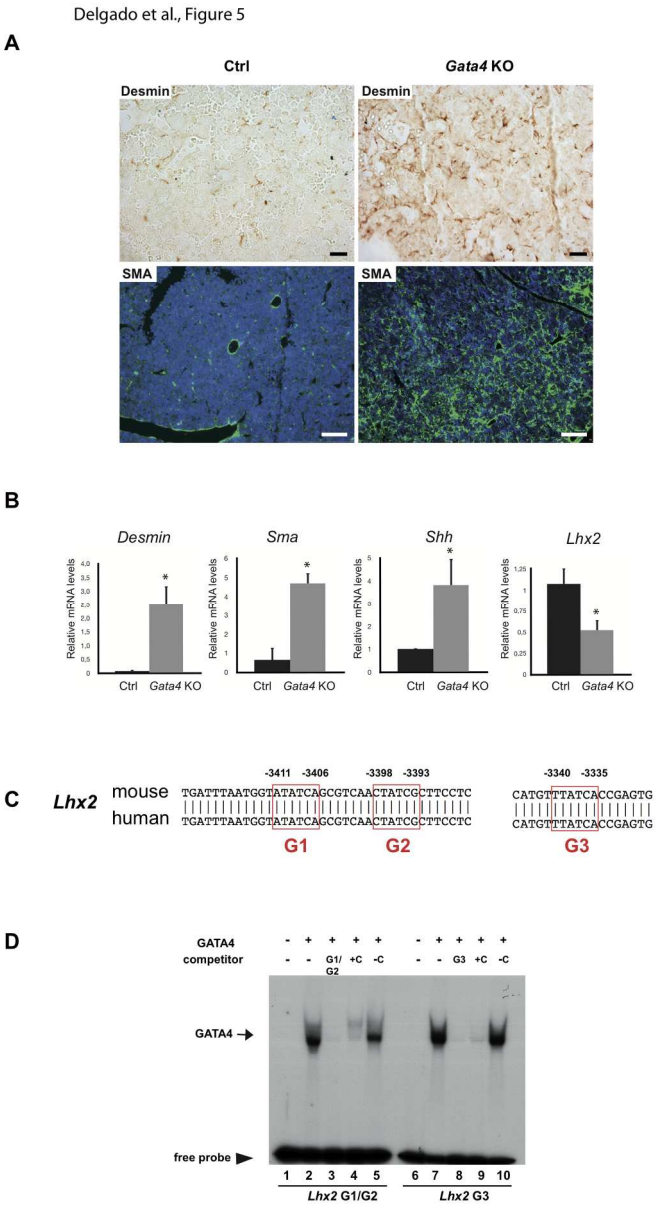

127x234mm (300 x 300 DPI)

Delgado et al., Figure 6

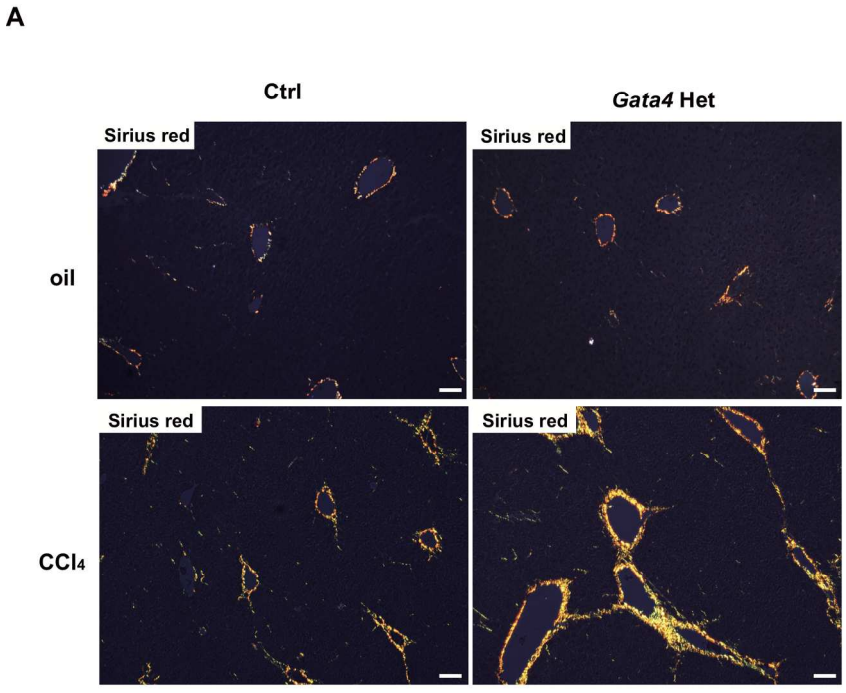

158x227mm (300 x 300 DPI)

Delgado et al., Figure 7

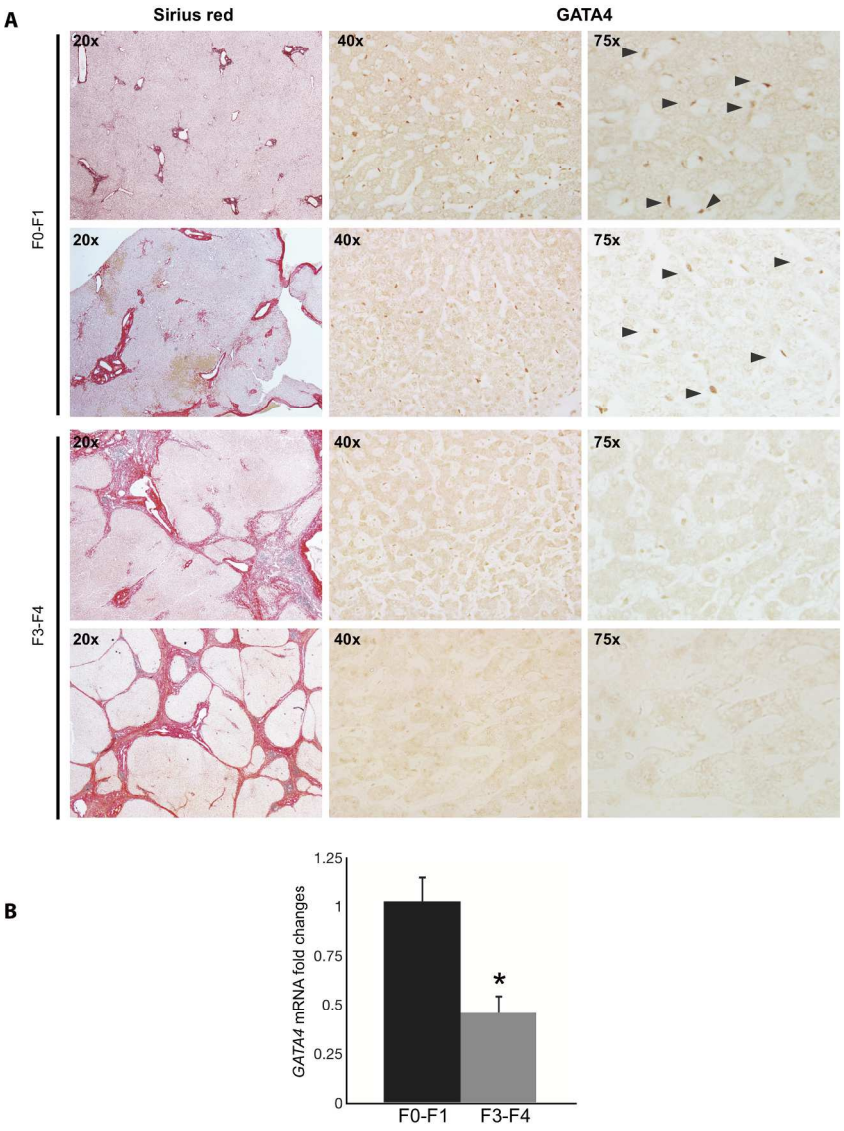

187x268mm (300 x 300 DPI)

Delgado et al., Supplemental Figure 1

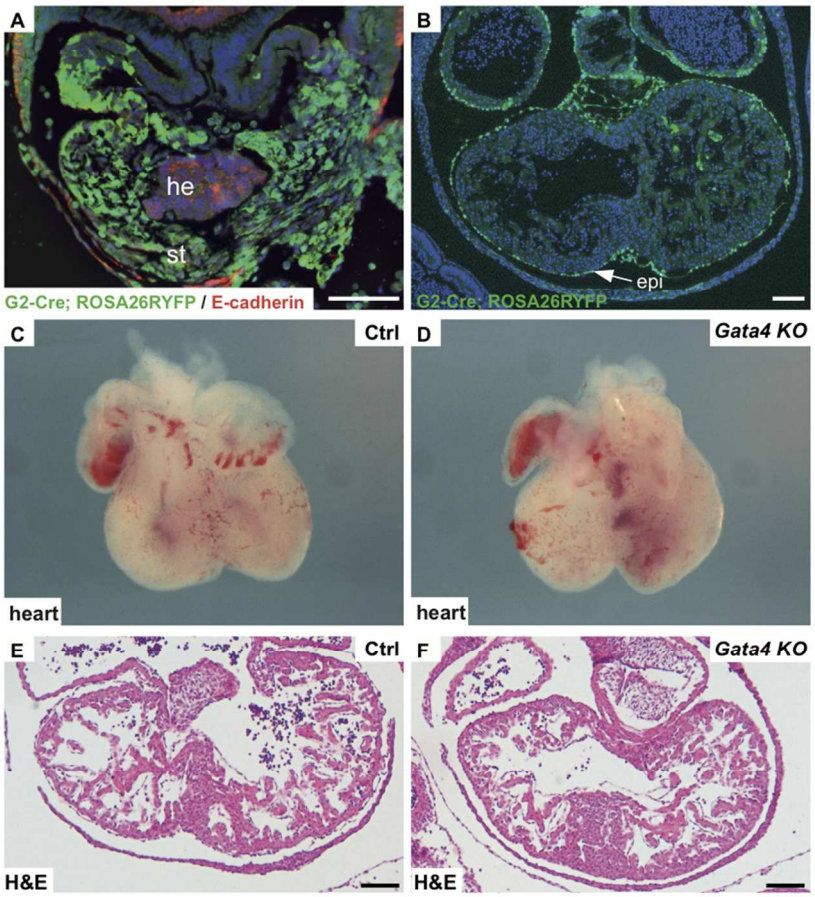

147x210mm (150 x 150 DPI)

Delgado et al., Supplemental Figure 2

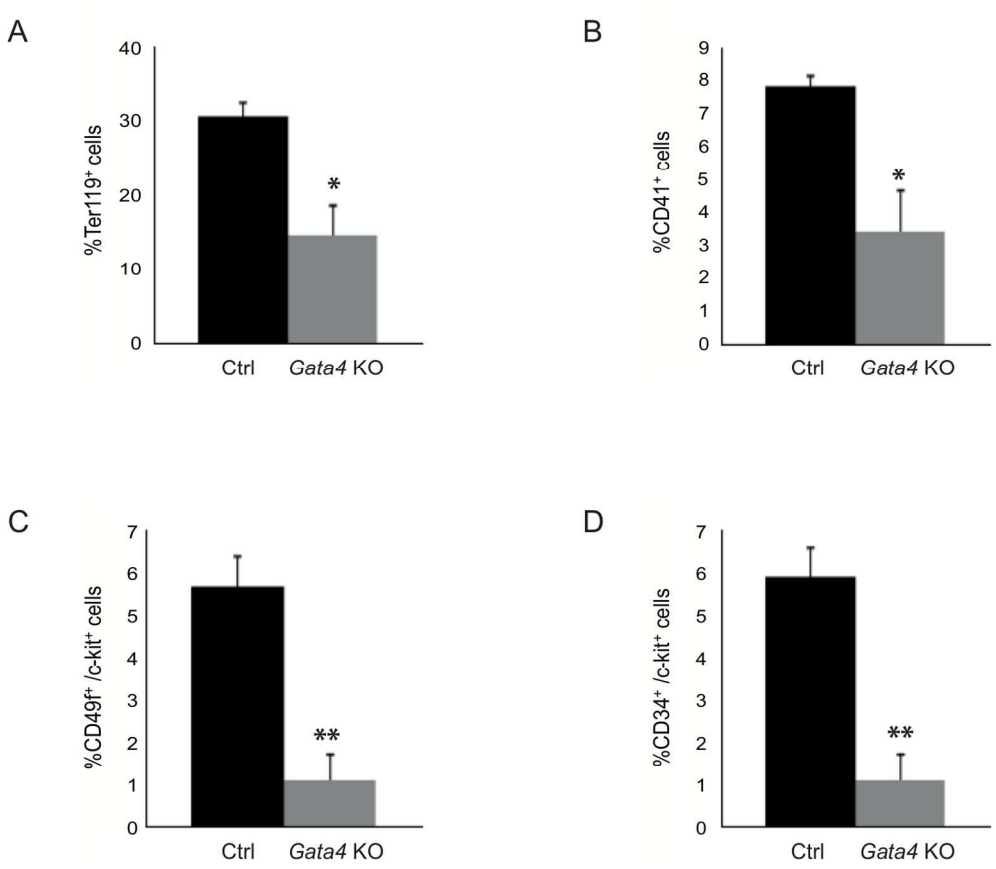

140x139mm (300 x 300 DPI)

Delgado et al., Supplemental Table 1

Table 1. Loss of GATA4 function in the septum transversum mesenchyme results in embryonic lethality

Genotype	E9.5	E11.5	E13.5	Newborn
$Gata4^{flox/flox}$	15 (30%)	39 (25%)	53 (25%)	69 (33%)
$Gata4^{flox/flox}$; Cre	13 (26%)	25 (16%)	19 (12%)	0
$Gata4^{flox/+}$	12 (24%)	46 (29%)	30 (21%)	86 (42%)
$Gata4^{flox/+}$; Cre	10 (20%)	45 (29%)	46 (31%)	48 (24%)
n=	50	155	148	203

Offspring of each genotype from E9.5 and E11.5 were present at normal Mendelian frequencies. By E13.5, the frecuency of *Gata4* conditional knockout mice were reduced compared to the expected frecuency (25%). No *Gata4* conditional knockouts in the STM were present at birth (Newborn).

Delgado et al., Supplemental Table 2

Supplemental Table 2. List of mouse primers used for qRT-PCR.

Gene	Sequences
Smooth muscle alpha actin	Forward: 5´- aaacaggaatacgacgaa-3´ Reverse: 5´- caggaatgatttggaaagga-3
Desmin	Forward: 5´-tacacctgcgagattgatgc-3´ Reverse: 5´-gtagcctcgctgacaacctc-3´
Shh	Forward: 5´-gctgtggaagcaggtttcg-3´ Reverse: 5´-ggaaggtgaggaagtcgct-3´
Lhx2	Forward: 5´-agcacacactttaaccatgccgacgt-3´ Reverse: 5´-attgtccgaagctggtggtgctt-3´

Supplemental Figure legends

Supplemental Figure 1. (A, B) Transverse sections of E9.5 (A) and E11.5 (B) G2-Cre; *ROSA26RYFP* embryos stained with anti-GFP antibody are shown. YFP+ cells are confined to the septum transversum and absent from the hepatic bud (he), marked by E-cadherin reactivity at E9.5 (A). Within the heart, YFP^+ cells are restricted to the epicardium at E11.5 (B). Whole mount (C, D) or sections stained with H&E (E, F) from control (Ctrl) (C, E) or *Gata4* conditional knockout (G4KO) (D, F) are shown. Scale bars= 100μm.

Supplemental Figure 2. Decreased hematopoetic cell progenitors in *Gata4* conditional knockout fetal liver. Flow cytometry was perfomed for E12.5 control (Ctrl) or *Gata4* conditional knockout mice (G4KO) livers. The livers were dissected and mechanically disaggregated by repeated pipetting. Cell suspensions were incubated with the antibodies in flow cytometry buffer for 20 min on ice, washed and analyzed in a Mo-Flo flow cytometer. Antibodies used were from eBioscience, Anti-human/mouse CD49f-PE (12-0495-81), anti-mouse CD117-CY5 (19-1171-81), anti-mouse CD41-PE (12-0411-81), anti-mouse Ter-119-PE-Cy5 (15-5921-81) and anti-mouse CD34-FITC (11-0341-81). * $p < 0.05$; **$p< 0.01$(Student's *t*-test).

Supplemental Table 1. Loss of GATA4 function in the derivatives of the septum transversum mesenchyme results in embryonic lethality by E13.5.

Gata4$^{flox/+}$*; Gata4 G2*-Cre mice were crossed to *Gata4*$^{flox/flox}$ mice, and the offspring were collected at the indicated developmental stages. Offspring of each genotype from E9.5 to E11.5 were present at normal Mendelian frequencies. By E13.5,

near half of the conditional knockout embryos lacked a heartbeat. No *Gata4* conditional knockouts were present at birth (Newborn).